GLUT12 deficiency during early development results in heart failure and a diabetic phenotype in zebrafish

Vanesa Jiménez-Amilburu[†], Susanne Jong-Raadsen[1], Jeroen Bakkers[2], Herman P Spaink and Rubén Marín-Juez[1]

Institute of Biology, Leiden University, PO Box 9502, 2300 RA Leiden, The Netherlands
[1]ZF-screens BV, J.H. Oortweg 19, 2333 CH Leiden, The Netherlands
[2]Hubrecht Institute-KNAW and University Medical Center Utrecht and Interuniversity, 3584 CT Utrecht, The Netherlands
[†]V Jiménez-Amilburu is now at Department of Developmental Genetics, Max Planck Institute for Heart and Lung Research, Ludwigstrasse 43, 61231 Bad Nauheim, Germany

Correspondence should be addressed to R Marín-Juez or H P Spaink
Emails
marinjuez@zfscreens.com or h.p.spaink@biology.leidenuniv.nl

Abstract

Cardiomyopathies-associated metabolic pathologies (e.g., type 2 diabetes and insulin resistance) are a leading cause of mortality. It is known that the association between these pathologies works in both directions, for which heart failure can lead to metabolic derangements such as insulin resistance. This intricate crosstalk exemplifies the importance of a fine coordination between one of the most energy-demanding organs and an equilibrated carbohydrate metabolism. In this light, to assist in the understanding of the role of insulin-regulated glucose transporters (GLUTs) and the development of cardiomyopathies, we have developed a model for *glut12* deficiency in zebrafish. GLUT12 is a novel insulin-regulated GLUT expressed in the main insulin-sensitive tissues, such as cardiac muscle, skeletal muscle, and adipose tissue. In this study, we show that *glut12* knockdown impacts the development of the embryonic heart resulting in abnormal valve formation. Moreover, *glut12*-deficient embryos also exhibited poor glycemic control. Glucose measurements showed that these larvae were hyperglycemic and resistant to insulin administration. Transcriptome analysis demonstrated that a number of genes known to be important in cardiac development and function as well as metabolic mediators were dysregulated in these larvae. These results indicate that *glut12* is an essential GLUT in the heart where the reduction in glucose uptake due to *glut12* deficiency leads to heart failure presumably due to the lack of glucose as energy substrate. In addition, the diabetic phenotype displayed by these larvae after *glut12* abrogation highlights the importance of this GLUT during early developmental stages.

Introduction

Cardiovascular pathologies are a leading cause of mortality (Pagidipati & Gaziano 2013). Heart failure constitutes the primary cause of death in developed countries and its occurrence increases rapidly in developing countries (Sliwa *et al.* 2005, Lopez *et al.* 2006). As the heart is one of the most energy demanding tissues, heart

Published by Bioscientifica Ltd.

failure is tightly correlated with alterations in cardiac metabolism. In this regard, pathologies impacting metabolism and leading to alterations in glycemic control present one of the main risk factors for developing heart failure (Haslam & James 2005). Specially, type 2 diabetes (T2D) is strongly associated with heart failure (Bell 2003a). Patients with T2D present an increased incidence of heart failure ranging from two- to fivefold higher than nondiabetic patients (Kannel & McGee 1979). The main insulin-regulated glucose transporter (GLUT) expressed in peripheral tissues such as cardiac and skeletal muscle and adipose tissue is GLUT4 (Scheepers et al. 2004). In the presence of insulin, GLUT4 translocates to the plasma membrane, mediating the postprandial glucose uptake. Surprisingly, Glut4-deficient mice did not develop hyperglycemia, and skeletal muscle tissue showed an increased glucose uptake in response to insulin (Katz et al. 1995, Stenbit et al. 1996), suggesting that there might be other insulin-sensitive GLUTs still to be identified. Interestingly, years later when it was discovered, it was found that a newly discovered GLUT named GLUT12 is expressed in the main insulin-sensitive tissues and shares motifs that are known to be important for the regulation of GLUT4 in response to insulin (Rogers et al. 2002). Moreover, Stuart et al. (2009) demonstrated that in human myoblasts insulin stimulates GLUT12 translocation to the plasma membrane via PI3-K, in the same manner as GLUT4. In this light, recent data have shown that transgenic mice overexpressing Glut12 improved peripheral insulin sensitivity, enhancing tissue-specific insulin-stimulated glucose uptake (Purcell et al. 2011). In the same work, despite that a significant enhancement of the glucose uptake by EDL, soleus, fat and heart was observed in transgenic mice overexpressing Glut12, the heart showed the mildest improvement of all the tissues analyzed, while these transgenic mice exhibited a twofold increase in cardiac GLUT12 protein levels, one of the highest together with the brain (Purcell et al. 2011). A possible explanation to these observations was presented recently by Waller et al. (2013) showing that in contrast to what happens in other tissues (i.e. skeletal muscle and adipose tissue) Glut12 might be functioning mainly as a basal GLUT in the heart.

These evidences indicate that further in-depth studies on the physiological role of GLUT12 will make important contributions to better understand the connection between heart failure and pathologies impacting the glucose metabolism.

In this work, we used zebrafish (Danio rerio) model to investigate the in vivo function of glut12. Zebrafish is a genetically tractable model that offers unique advantages for in vivo studies as well as a valuable tool to study diseases impacting metabolism (Seth et al. 2013). We demonstrate that zebrafish glut12 structure and tissue distribution are highly conserved and similar to its mammalian ortholog. In addition, we show how glut12 in zebrafish is regulated by insulin and AMPK. Making use of reverse genetic approaches, we induced knockdown of glut12 in zebrafish. Our results indicate that glucose uptake mediated by glut12 is essential for cardiac development because glut12-deficient embryos exhibited normal development but showed heart failure. Moreover, knockdown of glut12 led to insulin resistance and hyperglycemia being reminiscent of diabetic phenotypes. Taken together, our results indicate that glut12 is an essential GLUT in the heart where the reduction in glucose uptake due to glut12 deficiency leads to an impaired heart development. In addition, the metabolic features of the glut12 morphants indicate that glut12 is an important insulin-regulated GLUT, making it a promising tool to assist in the development of drugs for the treatment of diabetic cardiomyopathies.

Materials and methods

Zebrafish maintenance and lines

Zebrafish were reared and handled in compliance with the local animal welfare legislation and maintained according to standard protocols (http://zfin.org). In this work, zebrafish lines used included WT AB/TL, Tg(myl7:eGFP) (Huang et al. 2003), Tg(fli1:GFP) (Lawson & Weinstein 2002), and Tg(fabp10:dsRed;ela3l:GFP)^gz12 (Farooq et al. 2008), hereafter named as 2-Color Liver Insulin Acinar Pancreas (Tg(2CLIP)). For heart extraction, insulin injections and imaging embryos were previously anesthetized in egg water containing 0.02% buffered 3-aminobenzoic acid ethyl ester (Sigma).

Sequence alignments and molecular phylogenetic analysis

Multiple sequence alignments of the deduced amino acid sequence of the zebrafish Slc2a12 were performed using CLC Main Workbench 6.9.1 (CLC Bio A/S, Aarhus, Denmark, www.clcbio.com).

Phylogenetic relationships were inferred based on the deduced amino acid sequence for zebrafish Slc2a12, using the UPGMA method in CLC Main Workbench 6.9.1. For phylogenetic analysis, 5000 iterations were used to

Published by Bioscientifica Ltd.

generate a bootstrap consensus tree. We used Genomicus genome browser (Louis *et al.* 2013) to perform the syntenic analysis of the genomic regions carrying *glut12* loci in zebrafish compared with orthologs from other species of vertebrates.

Morpholino design and injections

To knockdown zebrafish *glut12*, two morpholino oligos (Gene Tools, LLC, Philomath, OR, USA) were designed, one of them blocking the translation of zebrafish *glut12* (5′-TGCATCCATGTTCTTCAAGCGTTGT-3′) and the other one targeting the splice acceptor site of exon 2 (5′-CCTTTCCCTAAATGACTAACCTGAT-3′). Morpholinos were reconstituted in RNAse-free water, according to manufacturer's instructions. A standard control morpholino (5′-CCTCTTACCTCAGTTACAATTTATA-3′) (Gene Tools, LLC) was injected at the same concentration as the *glut12* MOs. MOs were diluted to a concentration of 0.5 mM in 1× Danieau buffer (58 mM NaCl, 0.7 mM KCl, 0.4 mM MgSO$_4$, 0.6 mM Ca(NO$_3$)$_2$, 5.0 mM HEPES (pH 7.6)), and 1 nl was injected at the one-cell stage using a Femtojet injector (Eppendorf, Hamburg, Germany).

RNA isolation, cDNA synthesis, RT-PCR, and qPCR

The embryos were collected at different stages (24, 48, 72, 96, and 120 hpf), sampling 20 embryos per condition, using 1 ml of QIAzol Lysis Reagent (Qiagen) and stored at −80 °C until its isolation. Also, to study the tissue distribution of *slc2a12*, different tissues from adult zebrafish (brain, eye, heart, intestine, liver, muscle, ovary, skin, spleen, and testis) were carefully extracted. The zebrafish were killed using an overdose of anesthesia (tricaine) and stored in RNAlater solution at −80 °C until processed for RNA isolation. Total RNA was reverse transcribed into cDNA using IScript Reverse Transcriptase (Bio-Rad Laboratories B.V.). All samples were treated with RQ1 DNAse (Promega) to remove any residual genomic DNA. Conventional PCR was performed using DreamTaq Green DNA Polymerase (Thermo Scientific, Rockford, IL, USA), following manufacturer's indications. qPCR analysis was performed using iQ SYBR Green supermix (Bio-Rad Laboratories B.V.). The reactions were run in a iCycler Thermal Cycler (Bio-Rad Laboratories B.V.) using the following protocol: 3 min at 95 °C, followed by 40 cycles of 15 s denaturation at 95 °C and 30 s at the corresponding melting temperatures, and a final melting curve of 81 cycles from 55 °C to 95 °C (0.5 °C increments every 10 s).

mRNA expression levels were normalized against the expression of *ppia1* as a housekeeping gene. The primer sequences used in this study are given in Supplementary Table 1, see section on supplementary data given at the end of this article.

Purification of hearts from zebrafish embryos

Extraction of hearts from 48 and 72 hpf zebrafish embryos was accomplished as described previously (Burns & MacRae 2006). A total of 150–200 hearts were used per sample. After extraction the hearts were kept in QIAzol Lysis Reagent (Qiagen) at −80 °C until its RNA isolation.

Heartbeat rate and analysis

To quantify the length of the cardiac cycle in zebrafish embryos and to study the differences between heartbeat rate in *glut12* morphants and WT, a Hamamatsu C9300-221 high-speed CCD camera was used following the protocol described by Tessadori *et al.* (2012). To quantify heart rhythm, we drew kymographs for atrium or ventricle of WT and morphant embryos at 48 and 72 hpf. A total of 9–18 embryos were recorded for each condition and a total of 20 cardiac cycles were measured per embryo using ImageJ 64 (Rasband, W.S., ImageJ, U. S. National Institutes of Health, Bethesda, MD, USA, http://imagej.nih.gov/ij/, 1997–2014).

Insulin and metformin administration and glucose measurements

Insulin was injected into the zebrafish larvae as described previously (Marín-Juez *et al.* 2014*b*). For exposure to 250 μM metformin, zebrafish embryos were dechorionated at 48 hpf and treated with the compound for 48 h at 28 °C. Metformin was added to the water. Glucose measurements were performed using a fluorescence-based enzymatic detection kit (Biovision, Mountain View, CA, USA) as previously described (Jurczyk *et al.* 2011).

Imaging

Bright-field images were obtained using a Leica M165C stereomicroscope equipped with a DFC420C digital color camera (Leica Microsystems, Wetzlar, Germany). For fluorescent image acquisition, a Leica MZ16FA stereo fluorescence microscope equipped with a DFC420C digital color camera (Leica Microsystems) was used except in the case of fluorescent pictures of the valves, for which a Leica TCS SPE confocal laser scanning microscope

(Leica Microsystems) was used. Image analysis and Z-stacks projections were processed using ImageJ 64 (Rasband, W.S., ImageJ, U. S. National Institutes of Health, Bethesda, MD, USA, http://imagej.nih.gov/ij/, 1997–2014).

Transcriptome analysis

The WT embryos were injected with 0.5 mM of either standard control or splice *glut12* MO. Ten larvae per sample were pooled and three samples per condition were generated for the analysis. Briefly, 1 µg of RNA was isolated using TRIzol reagent (Life Technologies) and total RNA was extracted according to the manufacturer's instructions. RNA samples were treated with DNaseI (Life Technologies) to remove residual genomic DNA. RNA integrity was analyzed by Lab-on-a-chip analysis (Agilent, Amstelveen, The Netherlands). The average RIN value of the RNA samples was 9.7 with a minimum of 9.5. A total of 2 µg of RNA was used to make RNA-seq libraries using the Illumina TruSeq RNA Sample Preparation Kit v2 (Illumina, Inc., San Diego, CA, USA). In the manufacturer's instructions, two modifications were made. In the adapter ligation step, 1 µl (instead of 2.5 µl) adaptor was used. In the library size selection step, the library fragments were isolated using a double-Ampure XP purification with a 0.7x beads to library ratio (Beckman Coulter, Woerden, The Netherlands). The resulting mRNA-seq library was sequenced using an Illumina HiSeq2500 instrument (Illumina, Inc.) according to the manufacturer's description with a read length of 2×50 nucleotides. Image analysis and base calling were done by the Illumina HCS version 2.0.12. Data analysis was performed using Genetiles software (www.genetiles.com, W J Veneman, J de Sonneville, K J van der Kolk, A Ordas, Z Al-Ars, A H Meijer and H P Spaink 2014, unpublished observations). False discovery rate (FDR)-adjusted *P* values were calculated based on the algorithm of Benjamini & Hochberg (1995). The raw RNA-seq data have been deposited in the NCBI GEO database under accession number GSE59683. Gene ontology (GO) analysis was performed with DAVID Bioinformatics Resources 6.7 (Dennis *et al.* 2003).

Statistical analyses

Statistical differences were analyzed with Prism 6.0 (GraphPad Software, San Diego, CA, USA) using *t*-test for comparisons between two groups and one-way ANOVA (with Tukey's *post hoc* test correction) for multiple group comparisons and considered to be significant at $P<0.05$.

Results

Characterization of zebrafish *glut12* ortholog

The zebrafish *glut12* gene maps to chromosome 12 and shares a high similarity with human *GLUT12* in its genomic sequence, both containing five exons (Supplementary Figure 3, see section on supplementary data given at the end of this article). Phylogenetic analysis to determine the conservation degree of the putative zebrafish Glut12 protein showed that it clustered with GLUT12 sequences from other vertebrates, being more closely related to human GLUT12 than to human GLUT10, another closely related Class 3 GLUT (Supplementary Figure 1A).

Comparison of the zebrafish Glut12-deduced amino acid sequence with those from other vertebrates showed a high percentage of sequence identity in all the cases (Supplementary Table 2, see section on supplementary data given at the end of this article and Supplementary Figure 1B). In addition, comparison of the genomic regions carrying the GLUT12 loci showed that the genes flanking zebrafish *glut12* are syntenic across the different species analyzed, confirming its orthology among vertebrates (Supplementary Figure 2A).

Next, to address whether tissue expression of zebrafish *glut12* is similar to that in humans using qPCR we analyzed the mRNA levels in a number of tissues extracted from adult zebrafish. This analysis revealed that, as in humans, zebrafish *glut12* expression is widely distributed over various organs with the highest expression levels in skeletal and cardiac muscles (Supplementary Figure 2B). It has been shown by *in situ* hybridization that *glut12* is expressed during the early development in the midbrain, eye, somites, and CNS (Thisse & Thisse 2004, Tseng *et al.* 2009). As we failed to reliably detect *glut12* expression in the embryonic heart by *in situ* hybridization, we extracted the hearts of zebrafish embryos at 48 and 72 hpf. RT-PCR analysis of the RNA extracted from these samples confirmed the expression of *glut12* in the zebrafish heart at these stages (Supplementary Figure 2C).

Insulin and metformin stimulate *glut12* expression

Human GLUT12 translocation to the plasma membrane in skeletal muscle is stimulated by insulin (Stuart *et al.* 2009). To better characterize the mechanisms regulating zebrafish *glut12*, we stimulated zebrafish larvae with insulin using a newly developed technique (Marín-Juez *et al.* 2014*b*). Zebrafish larvae at 4 days post fertilization (dpf) were injected into the caudal aorta with 100 nM and
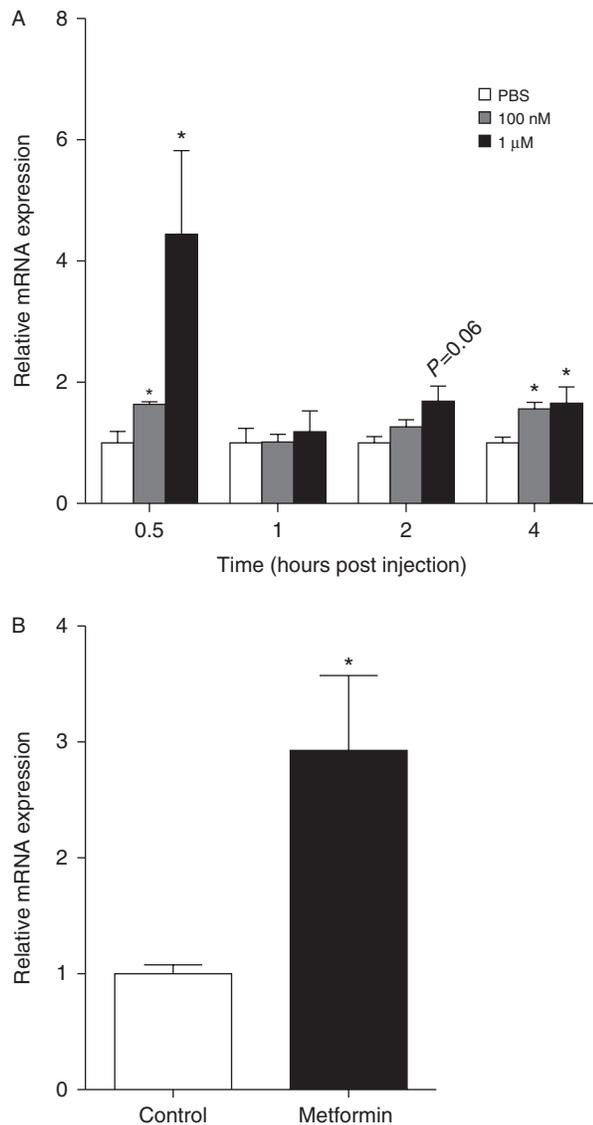
1 µM human recombinant insulin. qPCR analysis of *glut12* expression was performed in zebrafish larvae at 0.5, 1, 2, and 4 h post injection (hpi). Our results confirmed that injection of 100 nM or 1 µM insulin significantly stimulated *glut12* expression at 0.5 and 4 hpi (Fig. 1A). In mammals, *GLUT4* transcription is known to be stimulated

via AMP-activated protein kinase (AMPK; Jorgensen *et al.* 2006). As *glut4* is not present in zebrafish (Tseng *et al.* 2009, Marín-Juez *et al.* 2014a), we hypothesized that zebrafish *glut12* may be functioning as the main insulin-regulated GLUT and therefore being regulated by similar mechanisms. To test this hypothesis, we stimulated zebrafish embryos with 250 µM metformin, an indirect AMPK activator (Zhou *et al.* 2001, Viollet *et al.* 2012). qPCR analysis confirmed that *glut12* expression was significantly stimulated after metformin administration, resembling observations of mammalian GLUT4 (Fig. 1B). These evidences suggest that zebrafish *glut12* expression is regulated via insulin and AMPK signaling pathways, supporting the notion that in the absence of *glut4*, *glut12* in zebrafish could be the main insulin-regulated GLUT.

glut12 deficiency causes impaired cardiac development

To further study its physiological role, we resorted to reverse genetic approaches to abrogate *glut12*. The knockdown was performed using an antisense morpholino designed to interfere with the splicing between exons 2 and 3 (splice MO) (Supplementary Figure 3A, see section on supplementary data given at the end of this article). To ensure the specificity of this morpholino, we also designed a translation-blocking morpholino (ATG MO) (Supplementary Figure 3A). The embryos injected with the splice MO developed normally with exception of the appearance of heart edema at 72 hpf (Fig. 2A) and onwards (Supplementary Figure 3B). This was phenocopied by embryos injected with the ATG MO, confirming the specificity of the phenotype (Fig. 2A). To assess the extent of the splice-blocking activity of the splice MO, we carried out RT-PCR analysis of zebrafish embryos injected either with the control or with the splice MO from 24 to 120 hpf. Our results confirmed the efficiency of the morpholino showing the appearance of an aberrant splice product at all the different stages studied (Fig. 2B). In view of its efficiency and the possibility to easily confirm the knockdown, we chose to use the splice MO (hereafter named *glut12* MO) for the rest of the study.

We then investigated whether the *glut12* deficiency might be causing alterations in the heart development prior to the appearance of the cardiac edema. For this purpose, we injected the *glut12* MO in Tg(myl7:eGFP) zebrafish, which allows *in vivo* visualization of myocardial cells. By 48 hpf, morphant embryos showed defects in chamber morphology, revealing that a large proportion of morphant embryos presented alterations in the loop formation exhibiting either abnormal (47%) or no looping

Figure 1

glut12 expression is stimulated by insulin and metformin. (A) Zebrafish larvae were injected with human recombinant insulin at 100 nM and 1 µM in the caudal aorta at 4 dpf. Control embryos were injected with PBS. RNA samples for qPCR analysis were taken at 0.5, 1, 2, and 4 h after injection and *glut12* mRNA levels were measured. (B) Relative *glut12* expression after the exposure to metformin for 48 h at 250 mM. Data (mean±s.e.m.) are derived from a combination of four biological replicates (*n*=5 larvae per group) and expressed relative to the control, which is set to 1. *Significant differences between treatments (*P*<0.05).

Published by Bioscientifica Ltd.
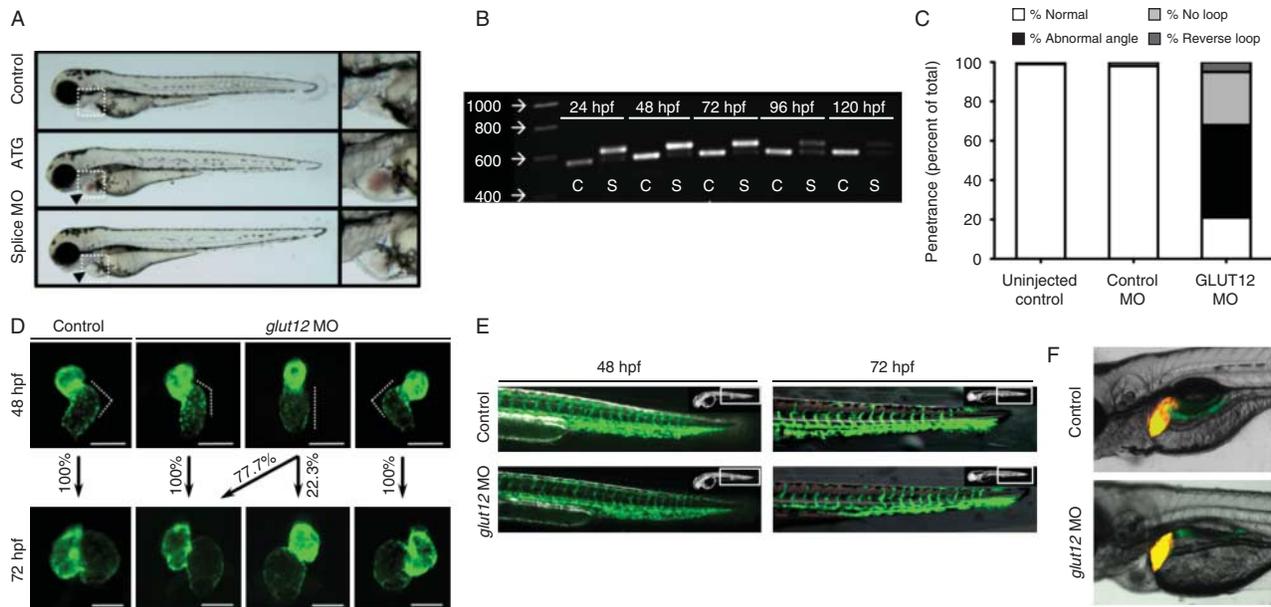
Figure 2

glut12 knockdown leads to impaired heart development. (A) Zebrafish embryos at 72 hpf injected with either ATG or control MOs exhibited heart edema (black arrowhead). White dotted boxes indicate the regions shown in the inserts. (B) RT-PCR analysis of larvae from 24 to 120 hpf injected with control and *glut12* MO to assess the extent of the splice-blocking activity of the splice MO. (C) The penetrance of the *glut12* knockdown was studied observing the different cardiac phenotypes present in the *Tg(myl7:eGFP)* embryos injected with the *glut12* MO. Phenotypes were classified according to the looping. (D) Further characterization of these embryos was carried out and the morphology of these hearts was studied at 72 hpf. 35 hearts of each type were analyzed. Scale bar indicates 150 μm. (E) *Tg(fli1:GFP)* embryos were injected with control and *glut12* MO and vasculature of the tail region was visualized at 48 and 72 hpf. (F) *Tg(2CLIP)* embryos were injected with the control and *glut12* MO. Liver (yellow–orange) and pancreas (green) were visualized at 96 hpf. A full colour version of this figure is available via http://dx.doi.org/10.1530/JOE-14-0539.

(27%) (Fig. 2C). In some cases reverse looping was observed, but despite that the incidence was slightly higher (5%), this phenomenon could be observed also in control embryos (2%) (Fig. 2C). The heart loop formation begins by approximately 36 hpf and is complete by 48 hpf (Bakkers 2011). This fact, together with the previous observations, led us to hypothesize that *glut12* deficiency would cause a reduction in glucose uptake by the heart, resulting in a reduced growth and proliferation of cardiac cells impairing the development of the heart. In this regard, to confirm that the observed phenotype was not restored after 48 hpf, we injected *Tg(myl7:eGFP)* with the *glut12* MO and followed larval heart development from 48 to 72 hpf. We observed that, while control and reversed loop hearts developed normally, hearts with abnormal looping angle at 48 and 72 hpf fail to loop, as a consequence the cardiac chambers fail to rotate, exhibiting a phenotype more similar to 48 hpf than to 72 hpf (Fig. 2D). Interestingly, hearts without loop at 48 hpf developed into the same phenotype as hearts with abnormal angle at 72 hpf, with a reduced percentage of them displaying the atrium in the reverse position (22.3%)

(Fig. 2D). To exclude the possibility that this could be due to alterations in the vasculature we injected *Tg(fli1:GFP)* with the *glut12* MO. We confirmed that the vascular system developed normally in morphant embryos from 24 to 72 hpf (Supplementary Figures 3C and 2E). In addition, we injected *Tg(2CLIP)* embryos with *glut12* MO, the results showing that the liver and the pancreas also developed normally (Fig. 2F). Overall, our results confirm that *glut12* deficiency alters heart development leading to the formation of an underdeveloped cardiac structure.

Loss of *glut12* leads to alterations in atrial and ventricular contraction resulting in arrhythmias

In view of the previous observations, we hypothesize that an underdeveloped heart may exhibit alterations in the heart rate and chamber contraction. To characterize these parameters, we analyzed the heart rhythm of *glut12* morphants by high-speed video imaging, quantifying heart rate and fractional sorting as described by Tessadori *et al.* (2012). As we observed that atrial and ventricle contractions were coupled in both control and morphant
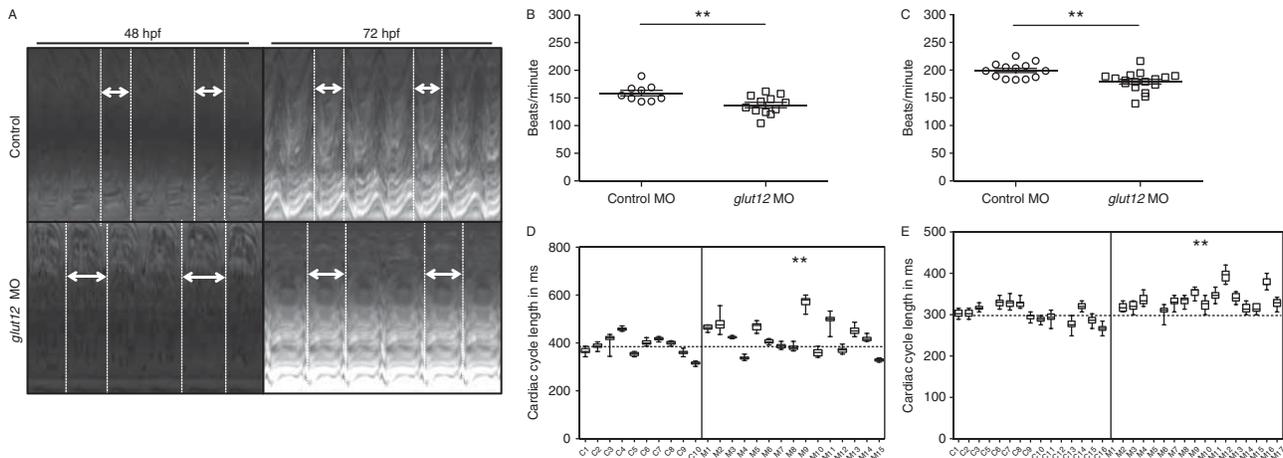
Figure 3

Cardiac contractility and rate are affected in *glut12* deficient embryos. High-speed imaging to count heartbeats was used in *glut12* morphants and control embryos. Embryonic hearts were imaged with a Hamamatsu C9300-221 high-speed CCD camera at 150 fps in a controlled temperature chamber (28.5 °C). Atrium kymographs from 48 and 72 hpf embryos were used to compare the length of cardiac cycle (period) in controls and *glut12* morphants. (A) The kymograph showed a longer period in morphants and embryos (data not shown), we performed all the high-speed imaging-based measurements in the atrium of zebrafish embryos at 48 and 72 hpf. Heart rhythm was quantified by kymographs obtained from the high-speed videos. These kymographs showed that the time required for a full cardiac cycle in *glut12* morphants was significantly extended (Fig. 3A). Next, based on these kymographs we quantified the cardiac cycle length and observed that the heart rate was significantly reduced (bradycardia) in *glut12* morphants at 48 and 72 hpf (Fig. 3B and C). In addition, cardiac length analysis confirmed the bradycardia and revealed irregular heart rhythm in *glut12* morphants that could be observed in some cases at 48 hpf (Fig. 3D) and clearly at 72 hpf (Fig. 3E). These observations indicate that the delayed cardiac development caused by the deficiency in *glut12* leads to heart failure.

was used to calculate the heart rate scatter dot plot representation of heartbeats per minute in 48 hpf (B) and 72 hpf (C) embryos. At least nine embryos per group were analyzed. Each dot represents one embryo. **$P < 0.01$. Box-whisker plot representation of the cardiac cycle length of 20 successive heartbeats at 48 hpf (D) and 72 hpf (E). Every box-plot represents one embryo. C, control; M, *glut12* morphants. **$P < 0.01$.

glut12 morphants exhibit blood toggling between heart chambers as a consequence of abnormal valve formation

Low heart rates have been described to lead to abnormal valve formation (Vermot *et al*. 2009). To investigate this effect, we analyzed high-speed imaging videos of control and *glut12* morphant embryos at 72 hpf, because at this stage valves should be fully formed preventing any retrograde flow fraction (RTT; Vermot *et al*. 2009). Interestingly, we observed that while in control embryos blood flow was unidirectional following atrial and ventricular contractions, morphant embryos exhibited blood toggling between the atrial systole and the ventricular diastole (Fig. 4A, Supplementary Movies 1 and 2, see section on supplementary data given at the end of this article). To confirm whether the alterations in heart rate affected valve morphogenesis in *glut12* morphants causing blood toggling, we used the *Tg(fli1:GFP)* line to visualize the valve formation at 72 hpf. While in control embryos we could observe the valves in between both cardiac chambers, these were absent in *glut12* morphants (Fig. 4B). Vermot *et al*. (2009) demonstrated that alterations in the heart rate cause valve dysgenesis via down-regulation of *klf2a*. To confirm this, we carried out qPCR analysis in hearts extracted from control and *glut12* morphant embryos at 72 hpf. Our results confirmed that *klf2a* expression was significantly down-regulated in morphant embryos (Fig. 4C). Taken together, these data indicate that the alterations in the heart rate as a consequence of the *glut12* deficiency down-regulate *klf2a* leading to abnormal valve formation.

Abrogation of *glut12* leads to hyperglycemia and insulin resistance

We set out to further investigate the physiological consequences of *glut12* abrogation. In view of the apparent
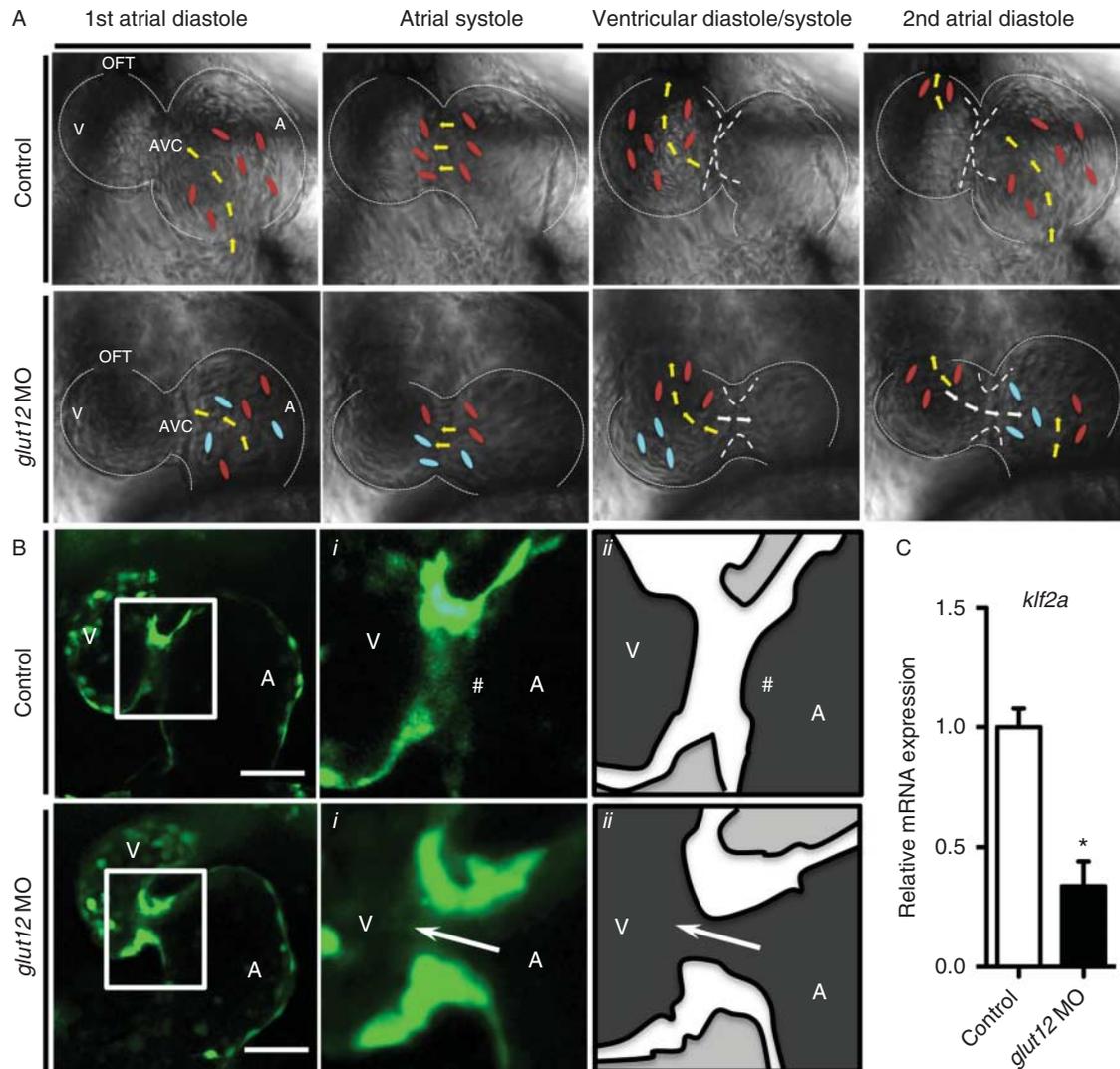
Figure 4

glut12 morphants exhibit backflows of blood as a consequence of abnormal valve formation. (A) Bright field images recorded by high-speed imaging comparing control and *glut12* morphant embryos showing a schematic representation of a cardiac cycle in zebrafish embryos. A zebrafish embryonic heart at 72 hpf is highlighted in white dotted contour and valves are highlighted in white dashed contour. Red ellipses, erythrocytes following normal flow; yellow arrows, normal blood flow; blue ellipses, erythrocytes fraction returning to the atrium; white arrows, blood backflow (For more detailed information see Supplementary Movies 1 and 2). (B) To better visualize the valve morphology in morphant embryos compared to the control we used *Tg(fli1:GFP)*. White boxes indicate the regions magnified in the sections *i* and *ii*. Scale bar indicates 50 μm. (*i*) High magnifications of the AVC regions. # indicates the closure of the AVC canal by the valves. The white arrow indicates the abnormal valve morphology and the consequent opening of the AVC. (*ii*) Schematic representation of the AVC regions. (C) Expression of *klf2a* was analyzed by qPCR. RNA was extracted from control and *glut12* morphants at 72 hpf. Data (mean ± s.e.m.) are combined from 4 biological replicates ($n = 150–200$ hearts per group) and expressed relative to control, which is set to 1. *$P < 0.05$. V, ventricle; A, atrium; AVC, atrio-ventricular canal; OFT, outflow tract. A full colour version of this figure is available via http://dx.doi.org/10.1530/JOE-14-0539.

lack of *glut4* in zebrafish and the previous observation indicating that insulin stimulates *glut12* expression, we hypothesize that a deficiency in *glut12* may lead to alterations in glycemic control of the larvae. To test this hypothesis, we measured free glucose levels in control and *glut12* MO injected embryos from 2 to 5 dpf.

In agreement with previous observations, free glucose levels appeared to diminish after 2 dpf, increasing again from 3 to 5 dpf (Jurczyk *et al*. 2011, Gut *et al*. 2013). This could correspond to an initial increase in glucose levels that might drive the maturation of beta pancreatic cells as observed in mammals (Hellerstrom & Swenne 1991,

Published by Bioscientifica Ltd.

Cao *et al*. 2004), dropping at 3dpf and increasing afterwards, coinciding with the functional onset of the hepatic gluconeogenesis (Gut *et al*. 2013). Our results showed that between 3 and 5 dpf, *glut12*-deficient embryos presented significantly higher free glucose levels (Fig. 5A). Next, to investigate whether the knockdown of *glut12* would be translated into a reduced insulin sensitivity, we measured free glucose levels in 4 dpf larvae at 15, 30, 60, and 120 min post injection of 1 nl of 100 nM human insulin. Interestingly, in *glut12*-morphant larvae, insulin administration caused no significant reduction in free glucose levels, in contrast to control embryos where the expected hypoglycemic effect was observed

Figure 5

Knockdown of *glut12* leads to hyperglycemia and insulin resistance. (A) Glucose dynamics of *glut12* morphants were studied and compared to control embryos. Samples for free glucose measurements were taken at 2, 3, 4 and 5 dpf. Data (mean±s.e.m.) are combined from five biological replicates ($n=10$ embryos per group). **$P<0.01$. (B) Control and *glut12* morphant larvae were injected with human recombinant insulin at 100 nM in the caudal aorta at 4 dpf. In each case PBS-injected larvae were used as control. Samples for glucose measurements were taken at 0, 15, 30, 45, 60 and 120 min after injection. Data (mean±s.e.m.) are combined from five biological replicates ($n=10$ embryos per group). **$P<0.01$.
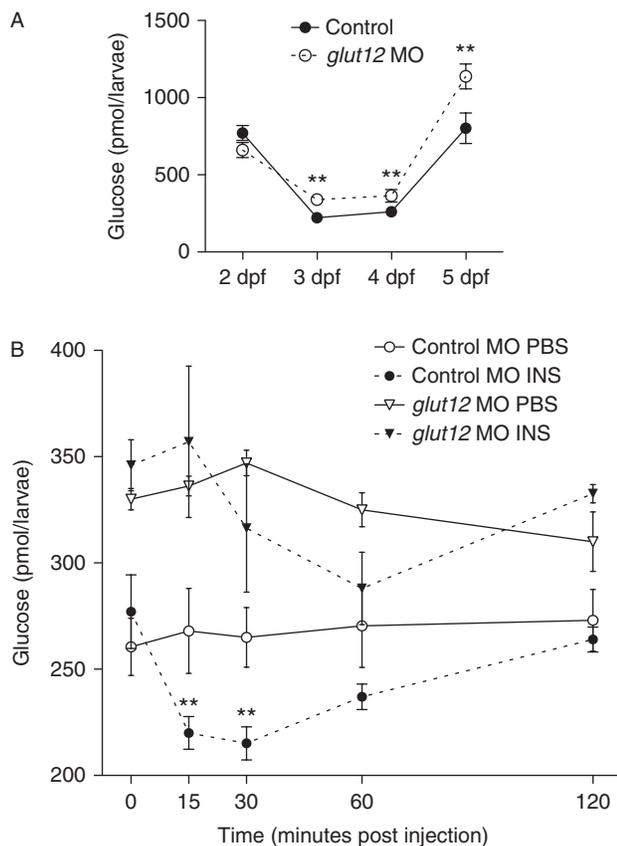
(Fig. 5B and Supplementary Figure 4, see section on supplementary data given at the end of this article).

Altogether, these data suggest that *glut12* abrogation causes a reduction in *glut12*-mediated glucose uptake causing hyperglycemia and insulin resistance, resembling a diabetic phenotype.

Transcriptomic profile confirms the observed cardiac and diabetic phenotype and reveals tissue-specific effects upon *glut12* knockdown

To better understand the impact of *glut12* deficiency at the whole embryo level, we carried out an RNAseq-based transcriptome analysis of 4 dpf *glut12*-morphant larvae compared with control larvae. To analyze the data, we set significance cut-offs at 1.5-fold change at $P<0.05$ (FDR adjusted P value). In this way, we obtained 1099 up-regulated genes and 290 down-regulated genes. Next, to further characterize the differentially expressed genes (DEGs), we performed a GO analysis for functional classification (Supplementary Tables 3, 4, and 5, see section on supplementary data given at the end of this article). In addition, RNA-seq data were validated by qPCR, observing the same effects on the expression of the genes analyzed by both techniques (Supplementary Figure 5, see section on supplementary data given at the end of this article).
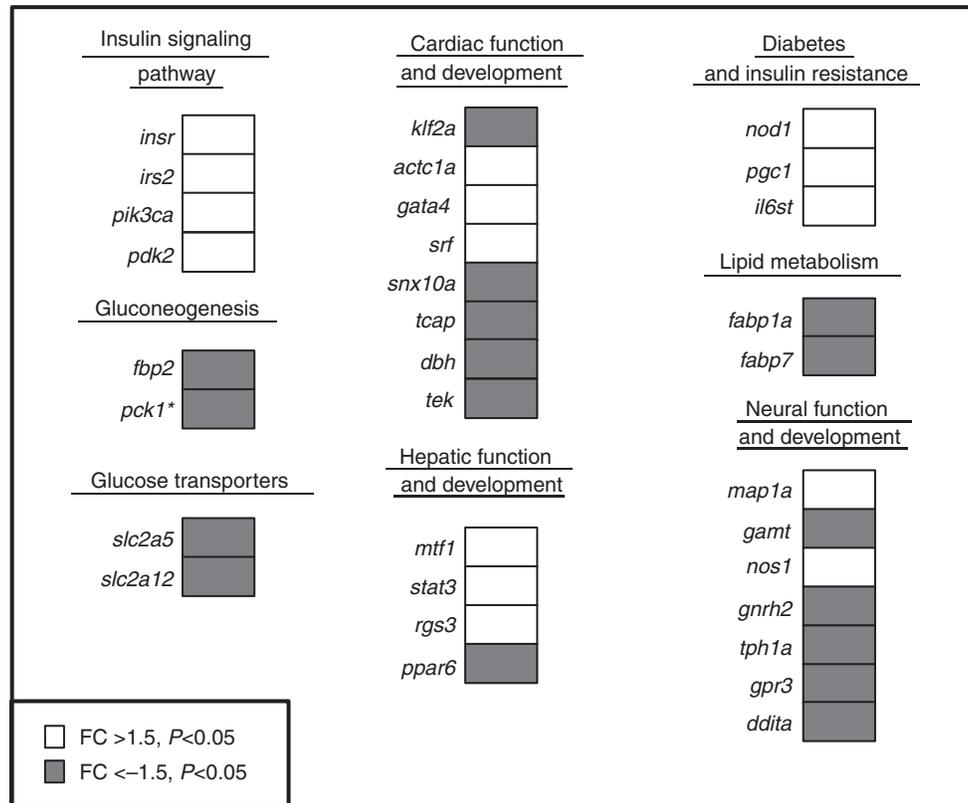
The study of GO terms showed that *glut12* deficiency altered biological processes involved in the development of the main organs responsible for glycemic control, which are commonly affected in diabetes (e.g., heart, liver, kidney, and skeletal muscle). In addition, other categories involving important pathways related to insulin signaling and action appeared dysregulated, such as the JAK–STAT and protein kinase cascades. When looking at cellular component and molecular function GO terms, we found an enrichment in categories involved in neural development. For more detailed analysis of the transcriptomic profile of the *glut12* morphants, we selected genes important for cardiac, hepatic, and neural function and development and insulin signaling pathway, as well as genes involved in metabolism and diabetes and/or insulin resistance (Fig. 6). Among DEGs involved in the insulin signaling pathway, a number of genes important to this pathway appeared up-regulated (*insr*, *irs2*, *pik3ca*, *pdk2*). Moreover, we observed a number of DEGs known to be important for the function and development of the heart (*klf2a*, *actc1a*, *gata4*, *srf*, *snx10a*, *tcap*, *dbh*, *tek*), liver (*mtf1*, *stat3*, *rgs3*, *ppar6*) and brain (*map1a*, *gamt*, *nos1*, *gnrh2*, *tph1a*, *gpr3*, *ddita*). Notably, we found that several genes known to be dysregulated in

Figure 6

Transcriptomic profile of *glut12*-deficient larvae. Transcriptomic analysis was performed comparing control and *glut12* morphants at 4 dpf. Grey boxes represent down-regulation and white boxes represent up-regulation. Significance cut-offs were set at fold change (FC) >1.5 and $P<0.05$. *Due to its relevance mediating a rate-limiting step of gluconeogenesis, *pck1* has been included in the figure despite its FC being 1.42 with a $P<0.05$.

diabetes or in insulin resistance (*nod1*, *pgc1*, *il6st*) were up-regulated in *glut12* morphants. Furthermore, genes involved in lipid metabolism (*fabp1a*, *fabp7*) and gluconeogenesis (*fbp2*, *pck1*) were down-regulated in *glut12*-deficient larvae. Finally, we found two GLUTs down-regulated *glut5* and *glut12*, the latter confirming the efficiency of the splice-blocking morpholino.

Discussion

Despite the fact that the heart can use a broad range of substrates as fuel, its metabolic machinery is finely regulated to ensure an optimal usage of the energy provided by these substrates. Aberrant metabolism is a common result of heart failure, for which cardiomyocytes resort to the usage of different substrates to fulfill the energetic needs of this metabolically demanding organ (van der Vusse *et al*. 2000, van Bilsen *et al*. 2004). Therefore, pathologies altering the control of metabolism (e.g., diabetes and insulin resistance) have critical

consequences contributing to the development and worsening of cardiomyopathies (Bell 2003*b*). One of the most recently discovered GLUTs, GLUT12, has been shown to be regulated by insulin in skeletal muscle (Stuart *et al*. 2009) and importantly has been described as a basal cardiac GLUT (Waller *et al*. 2013). Therefore, to gain insights into the physiological role of this GLUT, in this work we set out to study the functional consequences of *glut12* abrogation. As a result we could show how *glut12* abrogation impairs cardiac development, altering the contraction rate that in turns leads to alterations in the valvulogenesis. Moreover, we observed that *glut12*-deficient larvae were insulin resistant, exhibiting reduced insulin sensitivity and hyperglycemia, features characteristic of the diabetic phenotypes.

Both GLUT4 and GLUT12 have been shown to perform an important role in the cardiac muscle. Studies using a canine model for chronic heart failure showed that the expression of both *GLUT4* and *GLUT12* is affected in specific myocardial structures (Ware *et al*. 2011).

Moreover, *Glut4* deficiency in the heart has been reported to cause cardiomyopathies (Domenighetti *et al.* 2010). Supporting this notion, our data clearly show that the knockdown of *glut12* impairs embryonic heart development leading to alterations in contractility and bradycardia. Embryonic heart development is a tightly regulated process for which the energy source has been found to be a key determinant. During early development, cardiomyocyte precursors rely mainly on glycolysis to obtain energy (Chung *et al.* 2007, 2010). In addition, it has been described that proper heart formation is the result of a combination of genetic and mechanical factors that result in the proper development of the cardiac structures (Hove *et al.* 2003, Vermot *et al.* 2009). Valvulogenesis appears to be especially sensitive to alterations in this mechanogenetic equilibrium. Recently, Vermot *et al.* (2009) demonstrated that alterations in the RTT result in defective valve formation. Moreover, in the same study it was shown that variations in the heart rate lead to variations in the RTT via down-regulation of *klf2a*, causing valve dysgenesis as a consequence (Vermot *et al.* 2009). KLF2's responsiveness to the blood flow is well conserved

and it has been found expressed in regions subjected to high shear forces in human, chicken, and zebrafish hearts (e.g., the site of valve formation) (Dekker *et al.* 2002, Groenendijk *et al.* 2004, Vermot *et al.* 2009). As in mammals, *glut12* is found highly expressed in the heart of zebrafish and its abrogation resulted in clear alterations of the heart development probably as a consequence of the energy imbalance experienced by the cardiac muscle due to deficient glucose uptake. In view of this, we propose that the deficiency in glucose uptake caused by *glut12* abrogation impaired the embryonic heart development altering the loop formation, the contractility of myocardial cells, and the heart rate. This, in turn, altered the shear forces in the cardiac endothelium causing *klf2a* down-regulation and as a consequence valve dysgenesis (Fig. 7). Moreover, our deep sequencing data confirmed the down-regulation of *klf2a* and showed that the expression of a number of genes important for cardiac functioning and development was affected. Interestingly, *gata4* appeared up-regulated in our data set. *Gata4* over-expression has been reported to cause cardiac hypertrophy (Liang *et al.* 2001). During physiological cardiac
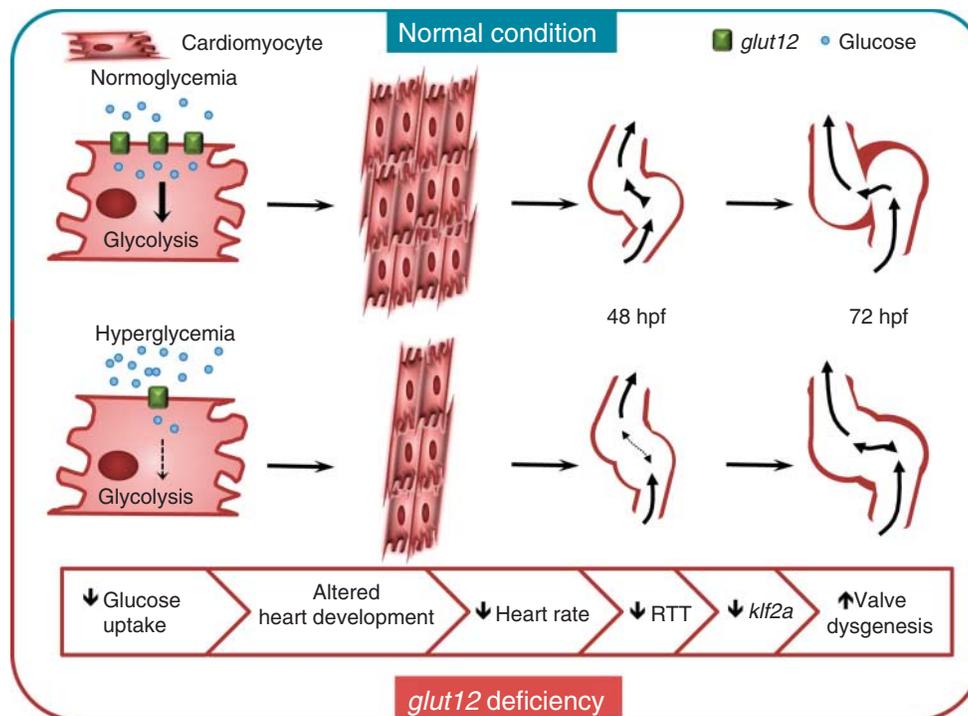
Figure 7

Proposed model for cardiac *glut12* deficiency. Cardiac glucose uptake is reduced as a consequence of the *glut12* abrogation. This impact on energy balance impairs the cardiac development altering the contractility of the myocardial cells and the heart rate. Embryonic hearts exhibiting poor looping and bradycardia have a reduced RTT down-regulating *klf2a*, which in turn causes valve dysgenesis. A full colour version of this figure is available via http://dx.doi.org/10.1530/JOE-14-0539.

hypertrophy, cardiac metabolism switches from glycolysis to fatty acid β-oxidation as the main source of energy (Lorell & Grossman 1987). However, in adult hearts experiencing pathophysiological hypertrophy, cardiac metabolism reverts to glycolytic metabolism resembling the fetal scenario (Lorell & Grossman 1987, Depre *et al.* 1998, Razeghi *et al.* 2001). In our case, *gata4* up-regulation in *glut12* morphants could reflect an attempt to switch to a less glucose-dependent cardiac metabolism. In our opinion, a scenario where *gata4* up-regulation may be reflecting pathological hypertrophy is most likely. The observed down-regulation in *glut12* morphants of *snx10a*, *dbh*, and *tek* supports this idea, because lack or deficiency of these genes has been reported to alter cardiac function, in some cases leading to heart failure (Swoap *et al.* 2004, Tachibana *et al.* 2005, Chen *et al.* 2012). We performed deep sequencing analysis at whole-embryo level to assess the global impact of *glut12* deficiency. Future transcriptomic studies focused on the heart in a tissue-specific manner will be needed to further study the observed phenotype.

GLUT12 has been proposed to be a secondary GLUT that complements GLUT4 mediating, insulin-stimulated glucose uptake (Stuart *et al.* 2009, Purcell *et al.* 2011). It has been shown that, in skeletal muscle, GLUT12 translocates to the plasma membrane together with GLUT4 after insulin stimulation (Stuart *et al.* 2009). These observations could also explain why *Glut4*-knock-out mice still showed insulin-stimulated glucose uptake and did not develop hyperglycemia (Katz *et al.* 1995, Stenbit *et al.* 1996). Moreover, Stenbit *et al.* showed later that *Glut4* heterozygote knockout mice displayed reduced insulin sensitivity in the skeletal muscle, hyperinsulinemia, and hyperglycemia (Stenbit *et al.* 1997). In this work, the authors propose that, while heterozygous mice have *Glut4* until the age of 8 weeks and then experience a decrease in *Glut4* content, *Glut4*-null mice have complete lack of the transporter developing and activating other mechanisms to compensate for this deficiency (Stenbit *et al.* 1997). One of these mechanisms could be *Glut12*.

Current data support the notion that in zebrafish *glut4* has been lost (Tseng *et al.* 2009, Marín-Juez *et al.* 2014a), making it an attractive model for the study of *glut12*, which could be functioning as the main insulin-regulated GLUT. Zebrafish *glut12* presents a high degree of conservation compared with its human counterpart in its protein structure, syntenic distribution, and tissue expression pattern. Moreover, our data also show that, in agreement with the observations in mammals, its

expression is regulated by insulin. Recently, it has been published by our group that human insulin is effective in zebrafish larvae (Marín-Juez *et al.* 2014b). In that work, we showed how 4 dpf larvae injected with 100 nM insulin experienced transient hypoglycemia between 15 and 45 min post injection, becoming insulin resistant at 4 hpi (Marín-Juez *et al.* 2014b). Interestingly, the expression of *glut12* is stimulated at 0.5 and 4 hpi, times at which zebrafish larvae are insulin sensitive and resistant respectively. The fast response observed at 0.5 hpi could indicate that *glut12* expression is rapidly stimulated in the presence of insulin to ensure an efficient glucose uptake. The latter stimulation could be explained as an attempt to compensate for the hyperglycemia that these larvae experience as a consequence of the hyper-insulinemia-induced insulin resistance that they experience at 4 hpi (Marín-Juez *et al.* 2014b).

As in mammals GLUT4 is known to be regulated by AMPK, we hypothesized that this could be the case for *glut12*, assuming that in zebrafish it is functioning as the main insulin-regulated GLUT in the absence of *glut4*. Our data showed that stimulation with the antidiabetic drug metformin, an indirect AMPK activator (Viollet *et al.* 2012), stimulates *glut12* expression, suggesting that like mammalian *GLUT4*, zebrafish *glut12* could be regulated via the AMPK signaling pathway. It is worth mentioning that because one of the main targets of metformin is the mitochondrial respiratory chain, it has been proposed that the activation of AMPK is a consequence of the energy imbalance that the cells experience when exposed to the drug (Viollet *et al.* 2012). In view of this, we cannot rule out the possibility that the observed effects might be due to AMPK-independent mechanisms. Future in-depth studies will help to elucidate this.

Interestingly, we show that *glut12* deficiency caused hyperglycemia and insulin resistance. These results are in agreement with recent data showing that mice overexpressing *Glut12* presented an improved insulin sensitivity (Purcell *et al.* 2011) and further support that in zebrafish *glut12* is an insulin regulated GLUT. In addition, the observed hyperglycemia might be a consequence of the reduced glucose uptake by tissues expressing *glut12*, especially the skeletal muscle since this represents a high portion of the larvae body mass.

The transcriptomic profiling showed that *nod1*, *il6st*, *srf* and *pgc1* were up-regulated in *glut12* morphants supporting the observed phenotype since activation in the case of *Nod1* or increased levels in the case of *Il6st* have been linked to insulin resistant states (Zuliani *et al.* 2010, Schertzer *et al.* 2011). Overexpression of *srf* is increased in

Published by Bioscientifica Ltd.

T2D but also has been reported to cause cardiomyopathy (Zhang *et al.* 2001) and *Pgc1α* dysregulation has been extensively studied and linked to T2D. However, in the case of *Pgc1α*, the observations differ in a tissue specific manner, observing *Pgc1α* up-regulation in the liver of mouse models for T1D and T2D (Puigserver & Spiegelman 2003), and down-regulation in muscle from humans with T2D (Mootha *et al.* 2003, Patti *et al.* 2003). Moreover, *Pgc1α* also plays a key role as a mediator of cardiac metabolism (Lehman *et al.* 2000, Arany *et al.* 2005). As noted before, future tissue specific studies will be helpful to elucidate the specific role of *pgc1* in a situation of *glut12* deficiency.

It is worth mentioning that our transcriptomic analysis also showed enrichment in DEGs involved in neural function and development. Interestingly, Pujol-Gimenez *et al.* (2014) found that *GLUT12* expression was increased in the frontal cortex of patients with Alzheimer disease, suggesting for the first time that GLUT12 might play a role in the development of Alzheimer disease.

In summary, in the present manuscript we demonstrate that *glut12* deficiency causes heart failure and diabetic phenotypes during embryonic development. In addition, it has been previously hypothesized that during early embryonic development, Glut12 might be the main GLUT responsible for insulin-regulated glucose uptake (Macheda *et al.* 2002) since *Glut4* is not expressed during early development, being only detectable at very low levels at late fetal/early postnatal life in mouse (Santalucia *et al.* 1992). In this regard, the zebrafish model for *glut12* deficiency that we used in this study will be a unique tool to not only study fetal diabetic cardiomyopathies but also contribute to the development and discovery of new anti-diabetic drugs thanks to its characteristics as a vertebrate model with high-throughput screening possibilities.

References

Arany Z, He H, Lin J, Hoyer K, Handschin C, Toka O, Ahmad F, Matsui T, Chin S, Wu PH *et al.* 2005 Transcriptional coactivator PGC-1 α controls the energy state and contractile function of cardiac muscle. *Cell Metabolism* **1** 259–271. (doi:10.1016/j.cmet.2005.03.002)

Bakkers J 2011 Zebrafish as a model to study cardiac development and human cardiac disease. *Cardiovascular Research* **91** 279–288. (doi:10.1093/cvr/cvr098)

Bell DS 2003*a* Diabetic cardiomyopathy. *Diabetes Care* **26** 2949–2951. (doi:10.2337/diacare.26.10.2949)

Bell DS 2003*b* Heart failure: the frequent, forgotten, and often fatal complication of diabetes. *Diabetes Care* **26** 2433–2441. (doi:10.2337/diacare.26.8.2433)

Benjamini Y & Hochberg Y 1995 Controlling the false discovery rate – a practical and powerful approach to multiple testing. *Journal of the Royal Statistical Society. Series B (Methodological)* **57** 289–300.

van Bilsen M, Smeets PJ, Gilde AJ & van der Vusse GJ 2004 Metabolic remodelling of the failing heart: the cardiac burn-out syndrome? *Cardiovascular Research* **61** 218–226. (doi:10.1016/j.cardiores.2003.11.014)

Burns CG & MacRae CA 2006 Purification of hearts from zebrafish embryos. *BioTechniques* **40** 274, 276, 278 passim. (doi:10.2144/000112135)

Cao LZ, Tang DQ, Horb ME, Li SW & Yang LJ 2004 High glucose is necessary for complete maturation of Pdx1-VP16-expressing hepatic cells into functional insulin-producing cells. *Diabetes* **53** 3168–3178. (doi:10.2337/diabetes.53.12.3168)

Chen Y, Wu B, Xu L, Li H, Xia J, Yin W, Li Z, Shi D, Li S, Lin S *et al.* 2012 A SNX10/V-ATPase pathway regulates ciliogenesis *in vitro* and *in vivo*. *Cell Research* **22** 333–345. (doi:10.1038/cr.2011.134)

Chung S, Dzeja PP, Faustino RS, Perez-Terzic C, Behfar A & Terzic A 2007 Mitochondrial oxidative metabolism is required for the cardiac differentiation of stem cells. *Nature Clinical Practice. Cardiovascular Medicine* **4**(Suppl 1) S60–S67. (doi:10.1038/ncpcardio0766)

Chung S, Arrell DK, Faustino RS, Terzic A & Dzeja PP 2010 Glycolytic network restructuring integral to the energetics of embryonic stem cell cardiac differentiation. *Journal of Molecular and Cellular Cardiology* **48** 725–734. (doi:10.1016/j.yjmcc.2009.12.014)

Dekker RJ, van Soest S, Fontijn RD, Salamanca S, de Groot PG, VanBavel E, Pannekoek H & Horrevoets AJ 2002 Prolonged fluid shear stress induces a distinct set of endothelial cell genes, most specifically lung Kruppel-like factor (KLF2). *Blood* **100** 1689–1698. (doi:10.1182/blood-2002-01-0046)

Journal of Endocrinology

Dennis G Jr, Sherman BT, Hosack DA, Yang J, Gao W, Lane HC & Lempicki RA 2003 DAVID: Database for Annotation, Visualization, and Integrated Discovery. *Genome Biology* **4** P3. (doi:10.1186/gb-2003-4-5-p3)

Depre C, Shipley GL, Chen W, Han Q, Doenst T, Moore ML, Stepkowski S, Davies PJ & Taegtmeyer H 1998 Unloaded heart *in vivo* replicates fetal gene expression of cardiac hypertrophy. *Nature Medicine* **4** 1269–1275. (doi:10.1038/3253)

Domenighetti AA, Danes VR, Curl CL, Favaloro JM, Proietto J & Delbridge LM 2010 Targeted GLUT-4 deficiency in the heart induces cardiomyocyte hypertrophy and impaired contractility linked with Ca(2+) and proton flux dysregulation. *Journal of Molecular and Cellular Cardiology* **48** 663–672. (doi:10.1016/j.yjmcc.2009.11.017)

Farooq M, Sulochana KN, Pan X, To J, Sheng D, Gong Z & Ge R 2008 Histone deacetylase 3 (hdac3) is specifically required for liver development in zebrafish. *Developmental Biology* **317** 336–353. (doi:10.1016/j.ydbio.2008.02.034)

Groenendijk BC, Hierck BP, Gittenberger-De Groot AC & Poelmann RE 2004 Development-related changes in the expression of shear stress responsive genes KLF-2, ET-1, and NOS-3 in the developing cardiovascular system of chicken embryos. *Developmental Dynamics* **230** 57–68. (doi:10.1002/dvdy.20029)

Gut P, Baeza-Raja B, Andersson O, Hasenkamp L, Hsiao J, Hesselson D, Akassoglou K, Verdin E, Hirschey MD & Stainier DY 2013 Whole-organism screening for gluconeogenesis identifies activators of fasting metabolism. *Nature Chemical Biology* **9** 97–104. (doi:10.1038/nchembio.1136)

Haslam DW & James WP 2005 Obesity. *Lancet* **366** 1197–1209. (doi:10.1016/S0140-6736(05)67483-1)

Hellerstrom C & Swenne I 1991 Functional maturation and proliferation of fetal pancreatic β-cells. *Diabetes* **40**(Suppl 2) 89–93. (doi:10.2337/diab.40.2.S89)

Hove JR, Koster RW, Forouhar AS, Acevedo-Bolton G, Fraser SE & Gharib M 2003 Intracardiac fluid forces are an essential epigenetic factor for embryonic cardiogenesis. *Nature* **421** 172–177. (doi:10.1038/nature01282)

Huang CJ, Tu CT, Hsiao CD, Hsieh FJ & Tsai HJ 2003 Germ-line transmission of a myocardium-specific GFP transgene reveals critical regulatory elements in the cardiac myosin light chain 2 promoter of zebrafish. *Developmental Dynamics* **228** 30–40. (doi:10.1002/dvdy.10356)

Jorgensen SB, Richter EA & Wojtaszewski JF 2006 Role of AMPK in skeletal muscle metabolic regulation and adaptation in relation to exercise. *Journal of Physiology* **574** 17–31. (doi:10.1113/jphysiol.2006.109942)

Jurczyk A, Roy N, Bajwa R, Gut P, Lipson K, Yang C, Covassin L, Racki WJ, Rossini AA, Phillips N *et al.* 2011 Dynamic glucoregulation and mammalian-like responses to metabolic and developmental disruption in zebrafish. *General and Comparative Endocrinology* **170** 334–345. (doi:10.1016/j.ygcen.2010.10.010)

Kannel WB & McGee DL 1979 Diabetes and cardiovascular disease. The Framingham study. *Journal of the American Medical Association* **241** 2035–2038. (doi:10.1001/jama.1979.03290450033020)

Katz EB, Stenbit AE, Hatton K, DePinho R & Charron MJ 1995 Cardiac and adipose tissue abnormalities but not diabetes in mice deficient in GLUT4. *Nature* **377** 151–155. (doi:10.1038/377151a0)

Lawson ND & Weinstein BM 2002 *In vivo* imaging of embryonic vascular development using transgenic zebrafish. *Developmental Biology* **248** 307–318. (doi:10.1006/dbio.2002.0711)

Lehman JJ, Barger PM, Kovacs A, Saffitz JE, Medeiros DM & Kelly DP 2000 Peroxisome proliferator-activated receptor gamma coactivator-1 promotes cardiac mitochondrial biogenesis. *Journal of Clinical Investigation* **106** 847–856. (doi:10.1172/JCI10268)

Liang Q, De Windt LJ, Witt SA, Kimball TR, Markham BE & Molkentin JD 2001 The transcription factors GATA4 and GATA6 regulate cardiomyocyte hypertrophy *in vitro* and *in vivo*. *Journal of Biological Chemistry* **276** 30245–30253. (doi:10.1074/jbc.M102174200)

Lopez AD, Mathers CD, Ezzati M, Jamison DT & Murray CJ 2006 Global and regional burden of disease and risk factors, 2001: systematic analysis of population health data. *Lancet* **367** 1747–1757. (doi:10.1016/S0140-6736(06)68770-9)

Lorell BH & Grossman W 1987 Cardiac hypertrophy: the consequences for diastole. *Journal of the American College of Cardiology* **9** 1189–1193. (doi:10.1016/S0735-1097(87)80326-1)

Louis A, Muffato M & Roest Crollius H 2013 Genomicus: five genome browsers for comparative genomics in eukaryota. *Nucleic Acids Research* **41** D700–D705. (doi:10.1093/nar/gks1156)

Macheda ML, Kelly DJ, Best JD & Rogers S 2002 Expression during rat fetal development of GLUT12 – a member of the class III hexose transporter family. *Anatomy and Embryology* **205** 441–452. (doi:10.1007/s00429-002-0263-8)

Marín-Juez R, Capilla E, Carvalho-Simoes F, Camps M & Planas JV 2014*a* Structural and functional evolution of glucose transporter 4 (GLUT4): a look at GLUT4 in fish. In *Glucose Homeostasis*. Ed L Szablewski. InTech: Rijeka, Croatia. (doi:10.5772/58094)

Marín-Juez R, Jong-Raadsen S, Yang S & Spaink HP 2014*b* Hyper-insulinemia induces insulin resistance and immune suppression via Ptpn6/Shp1 in zebrafish. *Journal of Endocrinology* **222** 229–241. (doi:10.1530/JOE-14-0178)

Mootha VK, Lindgren CM, Eriksson KF, Subramanian A, Sihag S, Lehar J, Puigserver P, Carlsson E, Ridderstrale M, Laurila E *et al.* 2003 PGC-1α-responsive genes involved in oxidative phosphorylation are coordinately downregulated in human diabetes. *Nature Genetics* **34** 267–273. (doi:10.1038/ng1180)

Pagidipati NJ & Gaziano TA 2013 Estimating deaths from cardiovascular disease: a review of global methodologies of mortality measurement. *Circulation* **127** 749–756. (doi:10.1161/CIRCULATIONAHA.112.128413)

Patti ME, Butte AJ, Crunkhorn S, Cusi K, Berria R, Kashyap S, Miyazaki Y, Kohane I, Costello M, Saccone R *et al.* 2003 Coordinated reduction of genes of oxidative metabolism in humans with insulin resistance and diabetes: potential role of PGC1 and NRF1. *PNAS* **100** 8466–8471. (doi:10.1073/pnas.1032913100)

Puigserver P & Spiegelman BM 2003 Peroxisome proliferator-activated receptor-γ coactivator 1 α (PGC-1 α): transcriptional coactivator and metabolic regulator. *Endocrine Reviews* **24** 78–90. (doi:10.1210/er.2002-0012)

Pujol-Gimenez J, Martisova E, Perez-Mediavilla A, Lostao MP & Ramirez MJ 2014 Expression of the glucose transporter GLUT12 in Alzheimer's disease patients. *Journal of Alzheimer's Disease* **42** 97–101. (doi:10.3233/JAD-132498)

Purcell SH, Aerni-Flessner LB, Willcockson AR, Diggs-Andrews KA, Fisher SJ & Moley KH 2011 Improved insulin sensitivity by GLUT12 over-expression in mice. *Diabetes* **60** 1478–1482. (doi:10.2337/db11-0033)

Razeghi P, Young ME, Alcorn JL, Moravec CS, Frazier OH & Taegtmeyer H 2001 Metabolic gene expression in fetal and failing human heart. *Circulation* **104** 2923–2931. (doi:10.1161/hc4901.100526)

Rogers S, Macheda ML, Docherty SE, Carty MD, Henderson MA, Soeller WC, Gibbs EM, James DE & Best JD 2002 Identification of a novel glucose transporter-like protein-GLUT-12. *American Journal of Physiology*. *Endocrinology and Metabolism* **282** E733–E738.

Santalucia T, Camps M, Castello A, Munoz P, Nuel A, Testar X, Palacin M & Zorzano A 1992 Developmental regulation of GLUT-1 (erythroid/Hep G2) and GLUT-4 (muscle/fat) glucose transporter expression in rat heart, skeletal muscle, and brown adipose tissue. *Endocrinology* **130** 837–846. (doi:10.1210/endo.130.2.1370797)

Scheepers A, Joost HG & Schurmann A 2004 The glucose transporter families SGLT and GLUT: molecular basis of normal and aberrant function. *JPEN. Journal of Parenteral and Enteral Nutrition* **28** 364–371. (doi:10.1177/0148607104028005364)

Schertzer JD, Tamrakar AK, Magalhaes JG, Pereira S, Bilan PJ, Fullerton MD, Liu Z, Steinberg GR, Giacca A, Philpott DJ *et al.* 2011 NOD1 activators link innate immunity to insulin resistance. *Diabetes* **60** 2206–2215. (doi:10.2337/db11-0004)

Seth A, Stemple DL & Barroso I 2013 The emerging use of zebrafish to model metabolic disease. *Disease Models & Mechanisms* **6** 1080–1088. (doi:10.1242/dmm.011346)

Sliwa K, Damasceno A & Mayosi BM 2005 Epidemiology and etiology of cardiomyopathy in Africa. *Circulation* **112** 3577–3583. (doi:10.1161/CIRCULATIONAHA.105.542894)

Stenbit AE, Burcelin R, Katz EB, Tsao TS, Gautier N, Charron MJ & Le Marchand-Brustel Y 1996 Diverse effects of Glut 4 ablation on glucose uptake and glycogen synthesis in red and white skeletal muscle. *Journal of Clinical Investigation* **98** 629–634. (doi:10.1172/JCI118833)

Stenbit AE, Tsao TS, Li J, Burcelin R, Geenen DL, Factor SM, Houseknecht K, Katz EB & Charron MJ 1997 GLUT4 heterozygous knockout mice develop muscle insulin resistance and diabetes. *Nature Medicine* **3** 1096–1101. (doi:10.1038/nm1097-1096)

Stuart CA, Howell ME, Zhang Y & Yin D 2009 Insulin-stimulated translocation of glucose transporter (GLUT) 12 parallels that of GLUT4 in normal muscle. *Journal of Clinical Endocrinology and Metabolism* **94** 3535–3542. (doi:10.1210/jc.2009-0162)

Swoap SJ, Weinshenker D, Palmiter RD & Garber G 2004 Dbh(−/−) mice are hypotensive, have altered circadian rhythms, and have abnormal responses to dieting and stress. *American Journal of Physiology. Regulatory, Integrative and Comparative Physiology* **286** R108–R113. (doi:10.1152/ajpregu.00405.2003)

Tachibana K, Jones N, Dumont DJ, Puri MC & Bernstein A 2005 Selective role of a distinct tyrosine residue on Tie2 in heart development and early hematopoiesis. *Molecular and Cellular Biology* **25** 4693–4702. (doi:10.1128/MCB.25.11.4693-4702.2005)

Tessadori F, van Weerd JH, Burkhard SB, Verkerk AO, de Pater E, Boukens BJ, Vink A, Christoffels VM & Bakkers J 2012 Identification and functional characterization of cardiac pacemaker cells in zebrafish. *PLoS ONE* **7** e47644. (doi:10.1371/journal.pone.0047644)

Thisse B & Thisse C 2004 Fast release clones: a high throughput expression analysis. *ZFIN Direct Data Submission* ZFIN ID: ZDB-PUB-040907-1. (available at: http://zfin.org/cgi-bin/webdriver?MIval=aa-pubview2.apg&OID=ZDB-PUB-040907-1)

Tseng YC, Chen RD, Lee JR, Liu ST, Lee SJ & Hwang PP 2009 Specific expression and regulation of glucose transporters in zebrafish ionocytes. *American Journal of Physiology. Regulatory, Integrative and Comparative Physiology* **297** R275–R290. (doi:10.1152/ajpregu.00180.2009)

Vermot J, Forouhar AS, Liebling M, Wu D, Plummer D, Gharib M & Fraser SE 2009 Reversing blood flows act through klf2a to ensure normal valvulogenesis in the developing heart. *PLoS Biology* **7** e1000246. (doi:10.1371/journal.pbio.1000246)

Viollet B, Guigas B, Sanz Garcia N, Leclerc J, Foretz M & Andreelli F 2012 Cellular and molecular mechanisms of metformin: an overview. *Clinical Science* **122** 253–270. (doi:10.1042/CS20110386)

van der Vusse GJ, van Bilsen M & Glatz JF 2000 Cardiac fatty acid uptake and transport in health and disease. *Cardiovascular Research* **45** 279–293. (doi:10.1016/S0008-6363(99)00263-1)

Waller AP, George M, Kalyanasundaram A, Kang C, Periasamy M, Hu K & Lacombe VA 2013 GLUT12 functions as a basal and insulin-independent glucose transporter in the heart. *Biochimica et Biophysica Acta* **1832** 121–127. (doi:10.1016/j.bbadis.2012.09.013)

Ware B, Bevier M, Nishijima Y, Rogers S, Carnes CA & Lacombe VA 2011 Chronic heart failure selectively induces regional heterogeneity of insulin-responsive glucose transporters. *American Journal of Physiology. Regulatory, Integrative and Comparative Physiology* **301** R1300–R1306. (doi:10.1152/ajpregu.00822.2010)

Zhang X, Azhar G, Chai J, Sheridan P, Nagano K, Brown T, Yang J, Khrapko K, Borras AM, Lawitts J et al. 2001 Cardiomyopathy in transgenic mice with cardiac-specific overexpression of serum response factor. *American Journal of Physiology. Heart and Circulatory Physiology* **280** H1782–H1792.

Zhou G, Myers R, Li Y, Chen Y, Shen X, Fenyk-Melody J, Wu M, Ventre J, Doebber T, Fujii N et al. 2001 Role of AMP-activated protein kinase in mechanism of metformin action. *Journal of Clinical Investigation* **108** 1167–1174. (doi:10.1172/JCI13505)

Zuliani G, Galvani M, Maggio M, Volpato S, Bandinelli S, Corsi AM, Lauretani F, Cherubini A, Guralnik JM, Fellin R et al. 2010 Plasma soluble gp130 levels are increased in older subjects with metabolic syndrome. The role of insulin resistance. *Atherosclerosis* **213** 319–324. (doi:10.1016/j.atherosclerosis.2010.08.074)